

Chapter 1

Why CMB Physics?

When approaching a new subject of study, especially within the realm of empirical sciences, the relevant question to ask is always the same: why should we learn about this? So, why should we learn about CMB physics? To answer this kind of questions one might be tempted to invoke either historical or subjective arguments. For instance one could say that, historically, blackbody emission is rather interesting in itself since it represented, at the dawn of the century, one of the fragile bridges that allowed us to pass from a classical description of macroscopic phenomena to the quantum mechanical language which is today the most appropriate for the discussion of microscopic physics. On a more aesthetic (and hence subjective) level, one could also affirm that blackbody emission is beautiful since it depends only upon one crucial parameter, i.e. the temperature. Subjectivity in science is very important since it drives the enthusiasm of researchers towards new and exciting fields of investigation. At the same time any subjective self-excitation should be gauged by more objective elements of judgment. Objectivity, for natural scientists, rhymes with testability. The quest for objectivity does not imply the lack of fantasy but, on the contrary, it just focuses our theoretical endeavor.

In this introductory chapter the theme will be to stress that there are objective elements that make CMB physics one of the most attractive and promising frameworks for gathering indirect informations on the early stages of the life of our own Universe. After a general introduction to blackbody emission, the motivations of this script will be spelled out. The bottom line will be that, indeed, the CMB is cosmological and represents the dominant component of the detected extra-galactic emission.

The whole observable Universe will therefore be approached, in the first approximation, as a system emitting electromagnetic radiation. The topics

to be treated in the present chapter are therefore the following:

- electromagnetic emission of the Universe;
- the blackbody spectrum;
- a bit of history of the CMB observations;
- the entropy of the CMB and its implications;
- the time evolution of the CMB temperature;
- a quick glance at the Sunyaev-Zeldovich effect.

All along this script the natural system of units will be adopted. In this system

$$\hbar = c = k_B = 1, \quad (1.1)$$

where $\hbar = h/2\pi$, c is the speed of light and k_B is the Boltzmann constant. In order to pass from one system of units to the other it is useful to recall that

- $\hbar c = 197.327 \text{ MeV fm}$;
- $K = 8.617 \times 10^{-5} \text{ eV}$;
- $(\hbar c)^2 = 0.389 \text{ GeV}^2 \text{ mbarn}$;
- $c = 2.99792 \times 10^{10} \text{ cm/sec}$.

In Fig. 1.1 a rather intriguing plot summarizes the electromagnetic emission of our own Universe. Only the extra-galactic emissions are reported.^a On the horizontal axis we have the logarithm of the energy of the photons (expressed in eV). On the vertical axis we reported the logarithm (to base 10) of $\Omega_\gamma(E)$ which is defined as

$$\Omega_\gamma(E) = \frac{1}{\rho_{\text{crit}}} \frac{d\rho_\gamma}{d \ln E}. \quad (1.2)$$

The specific form of $\Omega_\gamma(E)$ in the case of the CMB branch of the spectrum will be discussed in the following section (see, for instance, Eq. (1.12)). For the moment it suffices to note that $\Omega_\gamma(E)$ measures the energy density of the emitted radiation in critical units. The critical energy density ρ_{crit} can be understood, grossly speaking, as the mean energy density of the Universe, i.e. for the current values of the cosmological parameters, the energy density equivalent to about six proton masses per cubic meter (see, for instance, Eq. (1.11)).

^aBy extra-galactic emissions we mean radiation coming from the outside of our galaxy. Of course, as stressed later on, it must be borne in mind that our own galaxy is also an efficient emitter of electromagnetic radiation.

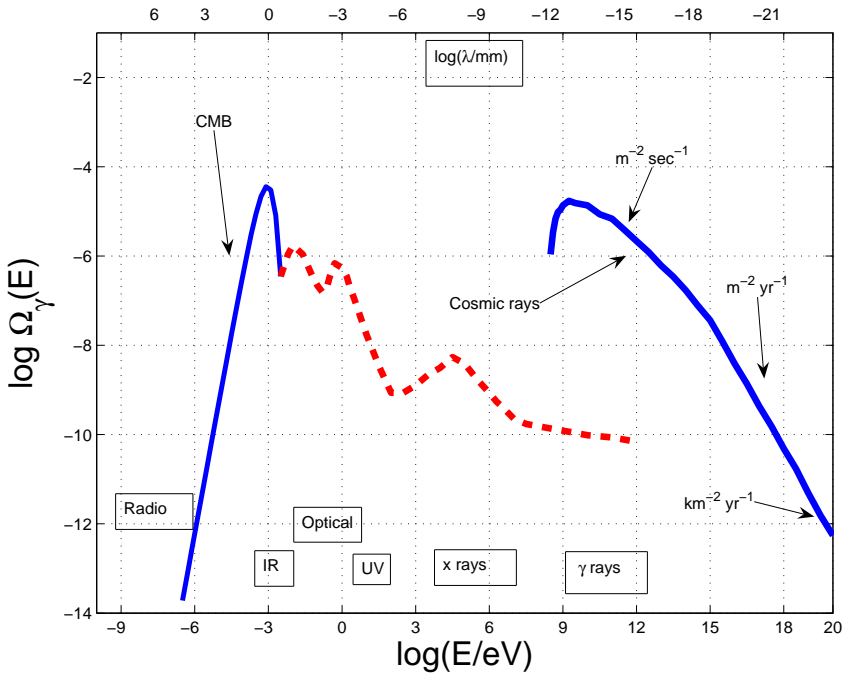


Fig. 1.1 In this cartoon the (extragalactic) electromagnetic emission is sketched. On the vertical axis the logarithm (to base 10) of the emitted energy density is reported in units of ρ_{crit} (see Eq. (1.9)). The logarithm of energy of the photons is instead reported on the horizontal axis. The wavelength scale is inserted at the top of the plot. The cosmic ray spectrum is included for comparison and in the same units used to describe the electromagnetic contribution.

For comparison also the associated wavelength of the emitted radiation is illustrated (see the top of the figure) in units of mm. Figure 1.1 motivates the choice of studying accurately the properties of CMB.

In Fig. 1.1 the maximum of $\Omega_\gamma(E)$ is located for a wavelength of the mm (see the scale of wavelengths at the top of Fig. 1.1) corresponding to typical energies of the order^b of 10^{-3} eV. In the optical and ultraviolet range of wavelengths the energy density drops almost two orders of magnitude. In the x -rays (i.e. 10^{-6} mm $< \lambda < 10^{-9}$ mm) the energy density of the emitted radiation drops more than three orders of magnitude in comparison with the maximum. The x -ray range corresponds to photon energies $E > \text{keV}$.

^bIn natural units $\hbar = c = k_B = 1$ we have $E_k = \hbar\omega = \hbar ck$ and that $k = 2\pi/\lambda$. So $E_k = k$ and $\omega = 2\pi\nu$.

In the γ -rays (i.e. 10^{-9} mm $<$ λ $<$ 10^{-12} mm) the spectral amplitude is roughly 5 orders of magnitude smaller than in the case of the millimeter maximum. The range of γ -rays occurs for photon energies $E >$ GeV. While the CMB represents 0.93 of the extragalactic emission, the infrared and visible part give, respectively, 0.05 and 0.02. The x -ray and γ -ray branches contribute, respectively, by 2.5×10^{-4} and 2.5×10^{-5} . The CMB is therefore the 93% of the total extragalactic emission. The CMB spectrum has been discovered by Penzias and Wilson [1] (see also [2]) and predicted, on the basis of the hot big-bang model, by Gamow, Alpher and Herman (see, for instance, [3]). Wavelengths as large as $\lambda \sim$ m lead to an emission which is highly anisotropic and will not be treated here as a cosmological probe. In any case, for $\lambda \geq$ m we are in the domain of the radio-waves. This branch of the spectrum is of upmost importance for a variety of problems including, for instance, large scale magnetic fields (both in galaxies and in clusters) [4] and pulsar astronomy [5]. In fact it should be mentioned that our own galaxy is also an efficient emitter of electromagnetic radiation. Since our galaxy possess a magnetic field, it emits synchrotron radiation as well as thermal bremsstrahlung. A very daring project that will probably be at the forefront of radio-astronomical investigations during the next 10 years is SKA (Square Kilometer Array) [6]. While the technical features of the instrument cannot be thoroughly discussed in the present script, it suffices to note that the collecting area of the instrument, as the name suggests will be of 10^6 m². The design of SKA will probably allow full sky surveys of Faraday rotation and better understanding of galactic emission.^c

In Fig. 1.1 the spectrum of the cosmic rays is also reported, for comparison. This inclusion is somehow arbitrary since the cosmic rays of moderate energy are known to come from within the galaxy. It is however useful to report also the energy spectrum of cosmic rays and to compare it, in the same units, with the energy spectrum of CMB photons. The energy density of the cosmic rays is, roughly, of the same order of the energy density of the CMB. For energies smaller than 10^{15} eV the rate is approximately of one particle per m² and per second. For energies larger than 10^{15} eV the rate is approximately of one particle per m² and per year. The difference in

^cWe will not enter here in the vast subject of CMB foregrounds. It suffices to appreciate that while the spectrum of synchrotron increases with frequency, for wavelengths shorter than the mm the emission is dominated by thermal dust emission whose typical spectrum decreases with frequency. It is opinion of the author that a better understanding of the spectral slope of the synchrotron would really be needed (not only from extrapolation). This seems important especially in the light of forthcoming satellite missions.

these two rates corresponds to a slightly different spectral behaviour of the cosmic ray spectrum, the so-called knee. Finally, for energies larger than 10^{18} eV, the rate of the so-called ultra-high-energy cosmic rays (UHECR) is even smaller and of the order of one particle per km^2 and per year. The sudden drop in the flux corresponds to another small change in the spectral behaviour, the so-called ankle. In the parametrization chosen in Fig. 1.1 the cosmic ray spectrum does not decrease as E^{-3} but rather as E^{-2} . The rationale for this difference stems from the fact that, in the parametrization of Fig. 1.1 we plot the energy density of cosmic rays per logarithmic interval of E while, in the standard parametrization the plot is in terms of $d\rho_{\text{crays}}/dE$. In the forthcoming years the spectrum above the ankle will be scrutinized by the AUGER experiment [7, 8]. While this book was in its final stages the preliminary results of the AUGER experiment appeared in a pair of papers, i.e. Refs. [9] and [10]. In [9] the collaboration achieved one decisive result for the spectrum of cosmic rays at energies in the range of the EeV. The hypothesis of the pure power law spectrum is rejected with a significance *better than 6 sigma and 4 sigma for minimum energies of $10^{18.6}$ eV and 10^{19} eV respectively* (verbatim from Ref. [9]). In [10] the data were analyzed to search for anisotropies near the direction of the galactic plane at EeV energies. The reported results suggest a highly isotropic distribution and *do not support previous findings of localized excesses in the AGASA and SUGAR data*^d (verbatim from the abstract of Ref. [10]).

The latest analyses of the AUGER experiment demonstrated a correlation between the arrival directions of cosmic rays with energy above 6×10^{19} eV and the positions of active galactic nuclei within 75 Mpc [11]. At smaller energies it has been convincingly demonstrated, as previously mentioned, that overdensities on windows of 5 deg radius (and for energies $10^{17.9}\text{eV} < E < 10^{18.5}\text{eV}$) are compatible with an isotropic distribution. The rejection of the hypothesis of a continuation of the spectrum in the form of a power-law is statistically significant [9]. The position of the ankle (i.e. the spectral break) occurs for $E_a \sim 10^{18.5}$ eV. The combined Auger spectrum can then be parametrized as

$$E^2\Omega_{\text{crays}}(E) \propto E^{3+\gamma_1}, \quad E < E_a,$$

$$E^2\Omega_{\text{crays}}(E) \propto E^{3+\gamma_2} \frac{1}{1 + \exp\left(\frac{\log E - \log E_c}{W_c}\right)}, \quad E > E_a, \quad (1.3)$$

^dAGASA and SUGAR data are former experiments analyzing cosmic rays in the EeV region.

where \log are base-10 logarithms and the energies are expressed in units of eV. In Eq. (1.3) γ_1 and γ_2 are the spectral index before and after the break respectively, E_a is the position of the break, and the second term in the second equation is a flux suppression term where E_c is the energy at which the flux is suppressed 50% compared to a pure power-law, and W_c determines the sharpness of the cutoff. Using Eq. (1.3) to fit the experimental data the collaboration obtains $\gamma_1 = -3.30 \pm 0.06$, $\gamma_2 = -2.56 \pm 0.06$, $\log E_a = 18.65 \pm 0.04$, $\log E_c = 19.74 \pm 0.06$ and $W_c = 0.16 \pm 0.04$. We point out that Eq. (1.3) is a parametrization, not a theoretical prediction. In spite of the fact that cosmic rays are not central to this presentation, we suggest the reader an interesting critical review on the theory of cosmic rays [12]. It is important to stress that while the CMB represents the 93 % of the extragalactic emission, the diffuse x -ray and γ -ray backgrounds are also of utmost importance for cosmology. Various experiments have been dedicated to the study of the x -ray background such as ARIEL, EINSTEIN, GINGA, ROSAT and, last but not least, BEPPO-SAX, an x -ray satellite named after Giuseppe (Beppo) Occhialini.^e Among γ -ray satellites we shall just mention COMPTON, EGRET and the forthcoming GLAST. In [13, 14] it was actually argued that the typical slope of the γ -ray background as measured by EGRET can be related to the slope of the cosmic ray spectrum.

1.1 The blackbody spectrum and its physical implications

According to Fig. 1.1, in the mm range the electromagnetic spectrum of the Universe is very well fitted by a blackbody spectrum: if we would plot the error bars magnified 400 times they would still be hardly distinguishable from the thickness of the curve. Starting from the discovery of Penzias and Wilson [1] various groups confirmed, independently, the blackbody nature of this emission (see below, in this section, for an oversimplified account of the intriguing history of CMB observations). As it is well known the blackbody has the property of depending only upon one single parameter which is the temperature T_γ of the photon gas. Such a temperature is given by

$$T_\gamma = 2.725 \pm 0.001 \text{ K.} \quad (1.4)$$

^ePart of the present book was prepared in connection with a PhD course at the University of Milan-Bicocca whose physics department is named after Giuseppe Occhialini.

According to Wien's law $\lambda T_\gamma = 2.897 \times 10^{-3}$ m K. Thus, as already remarked the wavelength of the maximum will be $\lambda \simeq$ mm. For a photon gas in thermodynamic equilibrium the energy density of the emitted radiation is given by

$$d\rho_\gamma = g \times \omega \times \frac{d^3\omega}{(2\pi)^3} \times \bar{n}_\omega, \quad (1.5)$$

where g is the number of intrinsic degrees of freedom ($g = 2$ in the case of photons) and n_ω is the Bose-Einstein occupation number :

$$\bar{n}_\omega = \frac{1}{e^{\omega/T_\gamma} - 1}. \quad (1.6)$$

Since in natural units, $E_k = k = \omega$, the energy density of the emitted radiation per logarithmic interval of frequency is given by:

$$\frac{d\rho_\gamma}{d \ln k} = \frac{1}{\pi^2} \frac{k^4}{e^{k/T_\gamma} - 1}. \quad (1.7)$$

Equation (1.7) allows also to compute the total (i.e. integrated) energy density ρ_γ . The differential spectrum of Eq. (1.7) can then be referred to the integrated energy density expressed, in turn, in units of the critical energy density. From Eq. (1.7) the integrated energy density of photons is simply given by

$$\rho_\gamma(t_0) = \frac{T_\gamma^4}{\pi^2} \int_0^\infty \frac{x^3}{e^x - 1} = \frac{\pi^2}{15} T_\gamma^4, \quad (1.8)$$

where the ratio $x = k/T_\gamma$ has been defined and where the integral in the second equality is given by $\pi^4/15$.

A useful way of measuring energy densities is to refer them to the *critical energy density* of the Universe (see chapter 2 for a more detailed discussion of this important quantity). In short we will also talk about critical density. According to the present data it seems that the critical energy density indeed coincides with the *total* energy density of the Universe. This is just because experimental data seem to favour a spatially flat Universe. The critical energy density today is given by^f:

$$\rho_{\text{crit}} = \frac{3H_0^2}{8\pi G} = 1.88 \times 10^{-29} h_0^2 \text{ g cm}^{-3} = 1.05 \times 10^{-5} h_0^2 \text{ GeV cm}^{-3}, \quad (1.9)$$

^fTo understand more physically the present value of the critical energy density we can say that the vacuum of a particle accelerator is of the order of 10^{-19} g cm⁻³. Furthermore, we can say that, prior to gravitational collapse, the mean density is of the order of the critical density. After gravitational collapse the mean matter density, for instance within the Milky way, is three or even four orders of magnitude larger than the critical density.

where h_0 (often assumed to be ~ 0.7 for the purpose of numerical estimates along this book) measures the indetermination on the present value of the Hubble parameter

$$H_0 = 100 \frac{\text{km}}{\text{sec Mpc}} h_0. \quad (1.10)$$

From the second equality appearing in Eq. (1.9), recalling that the proton mass is $m_p = 0.938 \text{ GeV}$, it is also possible to deduce

$$\rho_{\text{crit}} = 5.48 \left(\frac{h_0}{0.7} \right)^2 \frac{m_p}{\text{m}^3}, \quad (1.11)$$

showing that, the critical density is, grossly speaking, the equivalent of 6 proton masses per cubic meter. From Eqs. (1.7) and (1.9) we can obtain the energy density of photons per logarithmic interval of energy and in critical units, i.e.

$$\Omega_\gamma(k) = \frac{1}{\rho_{\text{crit}}} \frac{d\rho_\gamma}{d \ln k}. \quad (1.12)$$

Recalling that $E_k = k$ (and neglecting the subscript) we have that

$$\Omega_\gamma(E) = \frac{15}{\pi^4} \Omega_{\gamma_0} \frac{x^4}{e^x - 1}, \quad (1.13)$$

where

$$x = \frac{E}{T_\gamma} = 4.26 \times 10^3 \left(\frac{E}{\text{eV}} \right), \quad (1.14)$$

$$\Omega_{\gamma_0} = \frac{\rho_\gamma(t_0)}{\rho_{\text{crit}}} = 2.471 \times 10^{-5} h_0^{-2}.$$

The quantities $\Omega_\gamma(E)$ and Ω_{γ_0} are physically different:

- Ω_{γ_0} is the ratio between the total (present) energy density of CMB photons and the critical energy density; Ω_{γ_0} is independent on the frequency;
- $\Omega_\gamma(E)$ is the energy spectrum of CMB photons per logarithmic interval of frequency and expressed in critical units; $\Omega_\gamma(E)$, unlike Ω_{γ_0} , does depend on the frequency.

Crudely speaking (and up to numerical factors) Eq. (1.13) simply suggests that Ω_{γ_0} sets the overall normalization of $\Omega_\gamma(E)$. It can be explicitly verified that, inserting the numerical value of T_γ and ρ_c (i.e. Eqs. (1.4) and (1.9)), the figure of Eq. (1.14) is swiftly reproduced. The spectrum of Eq. (1.13) can be also plotted in terms of the frequency. Recalling that, in

natural units, $k = 2\pi\nu$ the parameter $x = k/T_\gamma$ can be directly expressed in terms of ν . Thus x can be easily written as:

$$x = \frac{k}{T_\gamma} = 0.01765 \left(\frac{\nu}{\text{GHz}} \right). \tag{1.15}$$

Consider now Eq. (1.13) and multiply both sides by h_0^2 . In this way the combination $h_0^2\Omega_{\gamma 0}$ will appear at the right hand side. This combination, as already remarked, does not depend on the indetermination of the Hubble constant. The logarithm (to base 10) of the obtained expression gives

$$\log h_0^2\Omega_\gamma(x) = \log \left(\frac{15}{\pi^4} \right) + \log h_0^2\Omega_{\gamma 0} + 4 \log x - \log [e^x - 1]. \tag{1.16}$$

If we now insert Eq. (1.15) inside Eq. (1.16) and plot the obtained expression as a function of ν/GHz , the curve reported in Fig. 1.2 will be swiftly obtained. It should be borne in mind that the CMB spectrum could be

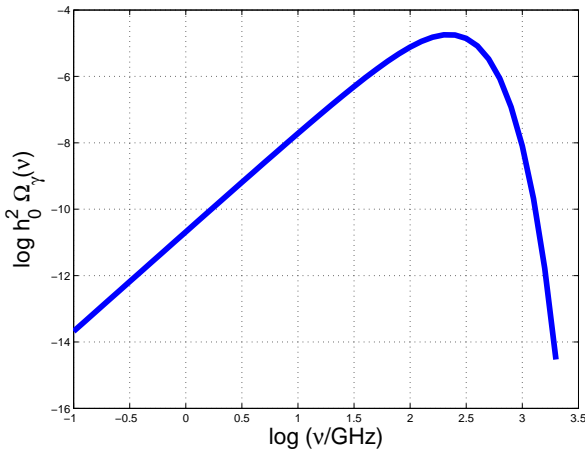


Fig. 1.2 The CMB logarithmic energy spectrum here illustrated in terms of the frequency.

distorted by several energy-releasing processes. These distortions have not been observed so far. In particular we could wonder if a sizable chemical potential is allowed. The presence of a chemical potential will affect the Bose-Einstein occupation number which will become, in our rescaled notations $\bar{n}_k^B = (e^{x+\mu_0} - 1)^{-1}$. The experimental data imply that $|\mu_0| < 9 \times 10^{-5}$ (95% C.L.). It is useful to mention, at this point, the energy density of the CMB in different units and to compare it directly with the cosmic ray spectrum as well as with the energy density of the galactic magnetic field. In

particular we will have

$$\rho_\gamma = \frac{\pi^2}{15} T_\gamma^4 = 2 \times 10^{-51} \left(\frac{T_\gamma}{2.725} \right)^4 \text{ GeV}^4, \quad (1.17)$$

$$\rho_B = \frac{B^2}{8\pi} = 1.36 \times 10^{-52} \left(\frac{B}{3\mu\text{G}} \right)^2 \text{ GeV}^4. \quad (1.18)$$

From Eqs. (1.17) and (1.18) it follows that the CMB energy density is roughly comparable with the magnetic energy density of the galaxy. Furthermore $\rho_{\text{crays}} \simeq \rho_B$.

1.2 A bit of history of CMB observations

The blackbody nature of CMB emission is one of the cornerstones of the Standard Cosmological Model^g whose essential features will be introduced in chapter 2. The first measurement of the CMB spectrum goes back to the work of Penzias and Wilson [1]. The Penzias and Wilson measurement referred to a wavelength of 7.35 cm (corresponding to 4.08 GHz). They estimated a temperature of 3.5 K. Since the Penzias and Wilson measurement the blackbody nature of the CMB spectrum has been investigated and confirmed for a wide range of frequencies extending from 0.6 GHz [16] (see also [17]) up to 300 GHz. The history of the measurements of the CMB temperature is a subject by itself which has been reviewed in the excellent book of B. Patridge [18]. Before 1990 the measurements of CMB properties have always been conducted through terrestrial antennas or even by means of balloon borne experiments. In the nineties the COBE satellite [19–26] allowed us to measure the properties of the CMB spectrum in a wide range of frequencies including the maximum (see Fig. 1.2). The COBE satellite had two instruments: FIRAS and DMR. The DMR was able to probe the angular power spectrum^h up to $\ell \simeq 26$. As the name implies, DMR was a differential instrument measuring temperature differences in the microwave sky. The angular resolution of a given instrument, i.e. ϑ , is related to the maximal multipole probed in the sky according to the approximate relation $\vartheta \simeq \pi/\ell$. Consequently:

^gIn this book the acronym SCM will often be used instead of standard cosmological model.

^hWhile the precise definition of angular power spectrum will be given later on, here it suffices to recall that $\ell(\ell + 1)C_\ell/(2\pi)$ measures the degree of inhomogeneity in the temperature distribution per logarithmic interval of ℓ . Consequently, a given multipole ℓ can be related to a given spatial structure in the microwave sky: small ℓ will correspond to low wavenumbers, high ℓ will correspond to larger wavenumbers.

- since the angular resolution of COBE was 7° , the maximal ℓ accessible to that experiment was $\ell \simeq 180^\circ/7^\circ \sim 26$;
- since the angular resolution of WMAPⁱ is 0.23° , the corresponding maximal harmonic probed by WMAP will be $\ell \simeq 180^\circ/0.23^\circ \sim 783$;
- finally, the Planck Explorer experiment,^j to be soon launched will achieve an angular resolution of $5'$, implying $\ell \simeq 180^\circ/5' \sim 2160$.

After the COBE mission, various experiments attempted the exploration of smaller angular separation, i.e. larger multipoles. A definite convincing evidence of the existence and location of the first peak in the C_ℓ spectrum came from the Boomerang [27, 28], Dasi [29] and Maxima [30] experiments. Both Boomerang and Maxima were balloon borne (bolometric) experiments. Dasi was a ground based interferometer. The data points of these last three experiments explored multipoles up to 1000, determining the first acoustic oscillation (in the jargon the first Doppler peak) for $\ell \simeq 220$. Another important balloon borne experiments was Archeops [31] providing interesting data for the region characterizing the first rise of the C_ℓ spectrum. Some other useful references on earlier CMB experiments can be found in [32]. The C_ℓ spectrum, as measured by different recent experiments is reported in Fig. 1.3 (adapted from Ref. [33]). At the moment the most accurate determinations of CMB observables are derived from the data of WMAP (Wilkinson Microwave Anisotropy Probe). The first release of WMAP data are the subject of Refs. [35–38]. The three-year release of WMAP data is discussed in Refs. [39, 40]. The WMAP data (filled circles in Fig. 1.3) provided, among other important pieces of information, the precise determination of the position of the first peak (i.e. $\ell = 220.1 \pm 0.8$ [36]) and evidence of the second peak. The WMAP experiment also measured temperature-polarization correlations providing a distinctive signature (the so-called anticorrelation peak in the temperature-polarization power spectrum for $\ell \sim 150$) of primordial adiabatic fluctuations (see chapters 8 and 9 and, in particular, Fig. 9.2). To have a more detailed picture of the

ⁱWMAP is the acronym for Wilkinson Microwave Anisotropy Probe and it is a satellite mission proposed to NASA in 1996 and launched in June 2001. Various experiments will be mentioned throughout this book and their essential features as well as the meaning of the corresponding acronym can be usefully obtained from the original references which are carefully quoted in the bibliographical section at the end of this book.

^jThe updated science case for the Planck experiment can be found at the following address <http://www.rssd.esa.int/index.php?project=PLANCK>. The long script that can be downloaded is often referred to, in the jargon, as the *Planck Bluebook*.

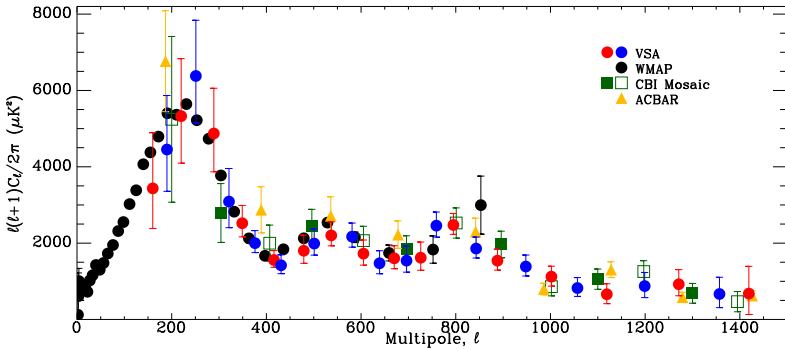


Fig. 1.3 Some CMB anisotropy data are reported (figure adapted from [33]): WMAP data (filled circles); VSA data (shaded circles) [34]; CBI data (squares) [41, 42]; ACBAR data (triangles) [43].

evolution and relevance of CMB experiments we refer the reader to Ref. [44] (for review of the pre-1994 status of the art) and Ref. [45] for a review of the pre-2002 situation). The rather broad set of lectures by Bond [46] may also be usefully consulted.

1.3 The entropy of the CMB and its implications

The pressure of blackbody photons is simply $p_\gamma = \rho_\gamma/3$. Since the chemical potential exactly vanishes in the case of a photon gas at the thermodynamic equilibrium, the entropy density of the blackbody is given, through the fundamental identity of thermodynamics (see Appendix B), by

$$s_\gamma = \frac{S_\gamma}{V} = \frac{\rho_\gamma + p_\gamma}{T_\gamma} = \frac{4}{45}\pi^2 T_\gamma^3, \quad (1.19)$$

where S_γ is the entropy and V is a fiducial volume. Equation (1.19) implies that the entropic content of the present Universe is dominated by the species that are relativistic today (i.e. photons) and that the total entropy contained in the Hubble volume, i.e. S_γ is *huge*. The Hubble volume can be thought of as the present size of our observable Universe and it is roughly given by $V_H = 4\pi H_0^{-3}/3$. Thus, we will have

$$S_\gamma = \frac{4}{3}\pi s_\gamma H_0^{-3} \simeq 1.43 \times 10^{88} \left(\frac{h_0}{0.7}\right)^{-3}. \quad (1.20)$$

The figure provided by Eq. (1.20) is still one of the major problems of the standard cosmological model. Why is the entropy of the observable

Universe so large? For the estimate of Eq. (1.20) it is practical to express both T_γ and H_0 in Planck units, namely^k:

$$T_\gamma = 1.923 \times 10^{-32} M_{\text{P}}, \quad H_0 = 1.22 \times 10^{-61} \left(\frac{h_0}{0.7} \right) M_{\text{P}}. \quad (1.21)$$

It is clear that the huge value of the present entropy is a direct consequence of the smallness of H_0 in Planck units. Equation (1.21) implies that $T_\gamma/H_0 \simeq 1.57 \times 10^{29}$. Let us just remark that the present estimate only concerns the thermodynamic entropy. Considerations related to the validity (also in the early Universe) of the second law of thermodynamics seem to suggest also that the entropy of the gravitational field itself may play a decisive role. While some motivations seem compelling there is no consensus, at the moment, on what should be the precise mathematical definition of the entropy of the gravitational field. This remark is necessary since we should keep our minds open. It may well be that the true entropy of the Universe (i.e. the entropy of the sources and of the gravitational field) is larger than the one computed in Eq. (1.20). Along this direction it is possible to think that the maximal entropy that can be stored inside the Hubble radius r_{H} is of the order of a black-hole with Schwartzchild radius $r_{\text{H}} \simeq H_0^{-1}$ which would give

$$r_{\text{H}}^2 M_{\text{P}}^2 \simeq 10^{122}. \quad (1.22)$$

In connection with Eq. (1.21), it is also useful to point out that the critical density can be expressed directly in terms of the fourth power of the Planck mass, i.e.:

$$\rho_{\text{crit}} = \frac{3}{8\pi} H_0^2 M_{\text{P}}^2 = 1.785 \times 10^{-123} \left(\frac{h_0}{0.7} \right)^2 M_{\text{P}}^4. \quad (1.23)$$

The huge hierarchy between the critical energy density of the present Universe and the Planckian energy density is, again, a direct reflection of the hierarchy between the Hubble parameter and the Planck mass. Such a hierarchy would not be, by itself, problematic. The rationale for such a statement is connected to the fact that in the SCM the energy densities as well as the related pressures decrease as the Universe expand. However, today, the largest portion of the energy density of the Universe is determined by a component called *dark energy*. The term *dark* is a coded word of astronomy. It means that a given form of matter or energy neither absorbs nor emit radiation. Furthermore the dark energy is homogeneously distributed

^kTo derive the second relation from the definition of H_0 (i.e. $H_0 = 100h_0 \text{ km sec}^{-1} \text{ Mpc}^{-1}$) it is practical to recall that $\text{Mpc} = 3.08 \times 10^{24} \text{ cm}$.

and, unlike *dark matter*, is not concentrated in the galactic halos and in the clusters of galaxies. One of the chief properties of dark energy is that it is not affected by the Universe expansion and this is the reason why it is usually parametrized in terms of a cosmological constant. Measurements tell us that $\rho_\Lambda \simeq 0.7\rho_{\text{crit}}$ which implies, from Eq. (1.23), that

$$\rho_\Lambda \simeq 1.24 \times 10^{-123} M_{\text{P}}^4. \quad (1.24)$$

Since ρ_Λ *does not* decrease with the expansion of the Universe, we have also to admit that Eq. (1.24) was enforced at any moment in the life of the Universe and, in particular, at the moment when the initial conditions of the SCM were set. A related way of phrasing this impasse relies on the field theoretical interpretation of the cosmological constant. In field theory we do know that the zero-point (vacuum) fluctuations have an energy density (per logarithmic interval of frequency) that goes as k^4 . Now, adopting the Planck mass as the ultraviolet cut-off we would be led to conclude that the total energy density of the zero-point vacuum fluctuations would be of the order of M_{P}^4 . On the contrary, the result of the measurements simply gives us a figure which is 122 orders of magnitude smaller.

The expression of the blackbody spectrum also allows the calculation of the photon concentration. Recalling that, in the case of photons, $dn = (k^3 n_k / \pi^2) d \log k$ we have, after integration over k that the concentration of photons is given by

$$n_{\gamma 0} = \frac{2\zeta(3)}{\pi^2} T_\gamma^3 \simeq 411 \text{ cm}^{-3} \quad (1.25)$$

where $\zeta(r)$ is the Riemann zeta function with argument r .

1.4 The time evolution of the CMB temperature

In summary we can therefore answer, in the first approximation, to the question giving the title of this chapter:

- in the electromagnetic spectrum the contribution of the CMB is by far larger than the other branches and constitutes, roughly speaking, 93 % of the whole emission;
- the CMB energy density is comparable with (but larger than) the energy density of cosmic rays;
- the CMB energy density is a tiny fraction of the total energy density of the Universe (more precisely 24 millionth of the critical energy density);

- the CMB dominates the total entropy of the present Hubble patch:
 $S_\gamma \simeq 10^{88}$.

The fact that we observe a CMB seems to imply that CMB photons are in thermal equilibrium at the temperature T_γ . This occurrence strongly suggests that the evolution of the whole Universe must somehow be adiabatic. In a preliminary perspective, the following naive observation is rather important. Suppose that the spatial coordinates expand thanks to a time-dependent rescaling. Consequently the wave-numbers will also be rescaled accordingly, i.e.

$$\vec{x}_0 \rightarrow \vec{x} = a(t)\vec{x}_0, \quad \vec{k}_0 \rightarrow \vec{k} = \frac{\vec{k}_0}{a(t)}. \quad (1.26)$$

In the jargon \vec{k}_0 is commonly referred to as the comoving wave-number (which is insensitive to the expansion), while \vec{k} is the physical wave-number. Consider then the number of photons contained in an infinitesimal element of the phase-space and suppose that the whole Universe expands according to Eq. (1.26). At a generic time t_1 we will then have

$$dn_k(t_1) = \bar{n}_k(t_1)d^3k_1d^3x_1. \quad (1.27)$$

At a generic time $t_2 > t_1$ we will have, similarly,

$$dn_k(t_2) = \bar{n}_k(t_2)d^3k_2d^3x_2. \quad (1.28)$$

By looking at Eqs. (1.27) and (1.28) it is rather easy to argue that $dn_k(t_1) = dn_k(t_2)$ provided $\bar{n}_k(t_1) = \bar{n}_k(t_2)$. By looking at the specific form of the Bose-Einstein occupation number it is clear that the latter occurrence is verified provided $k(t_1)/T_\gamma(t_1) = k(t_2)/T_\gamma(t_2)$. From this simple argument we can already argue an important fact: the blackbody distribution is preserved under the rescaling (1.26) provided the blackbody temperature evolves as the inverse of the scale factor $a(t)$, i.e.

$$T_{\gamma 0} \rightarrow T_\gamma = \frac{T_{\gamma 0}}{a(t)}. \quad (1.29)$$

The property summarized in Eq. (1.29) holds also in the context of the SCM where $a(t)$ will be correctly defined as the time-dependent scale factor of a Friedmann-Robertson-Walker (FRW) Universe. The physical consequence of Eq. (1.29) is that the temperature of CMB photons is higher at higher redshifts (see Appendix A for a definition of redshift). More precisely:

$$T_\gamma = (1+z)T_{\gamma 0}. \quad (1.30)$$

This consequence of the theory can be tested experimentally [47]. In short, the argument goes as follows. The CMB will populate excited levels of atomic and molecular species when the energy separations involved are not too different from the peak of the CMB emission. The first measurement of the local CMB temperature was actually made with this method by using the fine structure lines of CN (cyanogen) [48]. Using the same philosophy it is reasonable to expect that clouds of other chemical elements (like Carbon, in Ref. [47]) may be sensitive to CMB photons also at higher redshifts. For instance in [47] measurements were performed at $z = 1.776$ and the estimated temperature was found to be of the order of $T_\gamma(z) \simeq 7.5 \text{ }^0\text{K}$. These measurements are potentially very instructive but have been a bit neglected, in the recent past, since the attention of the community focused more on the properties of CMB anisotropies.

1.5 A quick glance to the Sunyaev-Zeldovich effect

For the limitations imposed by the introductory nature of the present script it is not possible to treat in detail the very interesting physics of another important effect that gives us valuable informations concerning the CMB and its primeval origin. It is in fact very important to establish empirically that CMB is not a merely local phenomenon, i.e. a phenomenon that arises in the local Universe. One definite answer, along this direction, is provided by the observation that, at higher redshifts, the putative CMB temperature indeed increases. The other definite answer comes exactly from the Sunyaev-Zeldovich (SZ) effect [49–51]. The physics of the SZ effect is, in a sense, rather simple. Clusters of galaxies have a deep potential well and on the average, by the virial theorem, their kinetic motion is of the order of few keV. So some fraction of the hot gas can get ionized and ionized plasma will be around. This plasma emits x -rays that, for instance, the ROSAT satellite has scutinized.¹ Now the CMB will sweep the whole space. By looking at a direction where there is nothing between the observer and the last scattering surface the radiation arrives basically unchanged except for the effect due to the expansion of the Universe. But if the observation

¹It is actually interesting, incidentally, that from the ROSAT full sky survey (allowing us to determine the surface brightness of various clusters in the x -rays), the average electron density has been determined [52] and this allowed interesting measurements of magnetic fields inside a sample of Abell clusters. The ROSAT satellite was an x -ray satellite flying from June 1990 to February 1999 and exploring the x -ray sky for energies between 0.1 keV and 2.4 keV.

is now made along a direction passing through a cluster of galaxies, some small fraction of the CMB photons (roughly one over 1000 CMB photons) will be scattered by the hot gas. Because the gas is actually hot, there is more probability that photons will be scattered at high energy rather than at low energy. They will also be scattered almost at isotropic angle. The bottom line is that the CMB spectrum along a line of sight that crosses a cluster of galaxies will have a slight excess of high energy photons and a slight deficiency of low energy photons. So if you see this effect (as we do) it means that the CMB photons come from behind the clusters. Some of these clusters are at redshift $0.07 < z < 1.03$. The measurements of the Sunyaev-Zeldovich effect have been attempted for roughly two decades but in the last decade a remarkable progress has been made. As already mentioned, the SZ effect tells that the CMB is really an extra-galactic radiation.

There are excellent long and short reviews on the SZ effect. Here we would like to quote just the classic review of Rephaeli [53] (see also [54]) as well as the non-relativistic treatments of the kinetic equation (which will be used in a moment to derive the non-relativistic expression of the modified spectral intensity) due to Kompaneets [55] (see also the comprehensive book of Peebles [56]). In what follows the simplest non-relativistic set-up will be described. The present treatment closely follows the one of Ref. [53] but within our set of conventions, units and definitions.

To give a simplified and self-contained introduction to the SZ effect, consider the following simplifications:

- assume first the Thompson limit where the frequency of the photons is much smaller than the electron mass; in this limit the cross section will simply be the Thompson cross section;
- derive the evolution of the Bose-Einstein occupation number in the non-relativistic limit where the kinetic equations reduce to the well known form of Fokker-Planck equation.

Using these two approximations we will have that the kinetic equation can be written as [55, 56]:

$$\frac{\partial \bar{n}_k}{\partial t} = \left(\frac{T_\gamma}{m_e} \right) \frac{\sigma_{\text{Th}} n_e}{x^2} \frac{\partial}{\partial x} \left[x^4 \left(\frac{T_e}{T_\gamma} \frac{\partial \bar{n}_k}{\partial x} + \bar{n}_k + \bar{n}_k^2 \right) \right], \quad (1.31)$$

where σ_{Th} is the Thompson cross section which will be discussed often in this book starting from chapter 2. In Eq. (1.31), T_γ is the photon temperature and T_e is the electron temperature. Since the temperature of the electrons of the cluster is large in comparison with the photon temperature

the following hierarchies hold:

$$\frac{T_e}{T_\gamma} \frac{\partial \bar{n}_k}{\partial x} \gg \bar{n}_k, \quad \frac{T_e}{T_\gamma} \frac{\partial \bar{n}_k}{\partial x} \gg \bar{n}_k^2. \quad (1.32)$$

Consequently Eq. (1.31) can be written as

$$\frac{\partial \bar{n}_k}{\partial t} = \frac{T_e}{m_e} \frac{\sigma_{\text{Th}} n_e}{x^2} \frac{\partial}{\partial x} \left(x^4 \frac{\partial \bar{n}_k}{\partial x} \right). \quad (1.33)$$

Equations (1.31) and (1.33) also assume that the distribution of the electrons is isotropic in the cluster frame. Now, if the incident radiation (i.e. the CMB) is only weakly scattered by the electrons, the approximate solution of Eq. (1.33) can be obtained by substituting at the right hand side of Eq. (1.33) the Bose-Einstein occupation number, i.e. $\bar{n}_k(x) = (e^x - 1)^{-1}$, and by then integrating along the line of sight to get the modified occupation number. The first step of this procedure leads to the following equation:

$$\frac{\partial \bar{n}_k}{\partial t} = \frac{T_e}{m_e} \sigma_{\text{Th}} n_e \mathcal{L}(x), \quad \mathcal{L}(x) = \frac{x[e^x(x-4) + (x+4)]}{(e^x - 1)^3} e^x. \quad (1.34)$$

Notice that the function $\mathcal{L}(x)$ goes to zero. In particular the zero of this function, i.e. $\mathcal{L}(x_0) = 0$ corresponds to $x_0 = 3.83$ which means, using Eq. (1.15) that connects x to ν in GHz units, $\nu_0 = 216.99$ GHz (often called crossover frequency). It is common practice, at this point, to work not with $h_0^2 \Omega_\gamma(\nu)$ but rather with the spectral intensity of the radiation field. There is no deep reason for doing that, however, for the sake of comparison with the notations customarily adopted in the literature we will stick to this convention and define the spectral intensity, in natural units as

$$I = \frac{T_\gamma^3}{2\pi^2} x^3 \bar{n}_k(x). \quad (1.35)$$

The scattered spectral intensity ΔI will then be obtained by integrating Eq. (1.33) along the line of sight with the result that

$$\Delta I = \frac{T_\gamma^3}{2\pi^2} g(x)y, \quad g(x) = x^3 \mathcal{L}(x) \quad (1.36)$$

where y is the Comptonization^m parameter, i.e.

$$y = \int \frac{T_e}{m_e} n_e \sigma_{\text{Th}} dL = \frac{T_e}{m_e} \sigma_{\text{Th}} \text{DM}. \quad (1.37)$$

In the second equality of Eq. (1.37), the so-called dispersion measurement $\text{DM} = \int n_e dL$ has been introduced.ⁿ The interesting exercise is now to take

^mThe COBE-FIRAS data set a bound to the Comptonization parameter which reads, to 95% confidence level, $|y| < 1.2 \times 10^{-5}$.

ⁿSometimes this quantity is also called column density of electrons.

the scattered radiation field given by Eq. (1.37), divide it by the spectral intensity in the absence of scattering (i.e. the spectral intensity of CMB photons that did not cross during their trajectory the hot electrons of a cluster) and evaluate the obtained expression in the limit $x \ll 1$ (which does correspond to the Rayleigh-Jeans region of the spectrum). The result of these simple manipulations is, therefore, the following:

$$\frac{\Delta I}{I} = C(x)y \simeq -2\left(1 + \frac{x}{2}\right)y, \tag{1.38}$$

$$C(x) = xe^x \frac{[(x-4)e^x + (x+4)]}{(e^x - 1)^2}$$

where the second equality defining $\Delta I/I$ follows in the limit $x \ll 1$. Equation (1.38) shows also the anticipated physics of the SZ effect: while the total photon concentration remains unchanged, photons are transferred from the Rayleigh-Jeans region to the Wien region, i.e. the final spectrum will have a slight deficiency of low-energy photons and a slight excess of high-energy photons.

The spectral change discussed so far had to do with the scattering of photons by hot electrons. It can also happen that the cluster has a peculiar velocity. In this case the modification of the spectral intensity will purely be kinematical and it will be given by [53]:

$$\Delta I = -\frac{T^3}{2\pi^2}h(x)v_r DM, \tag{1.39}$$

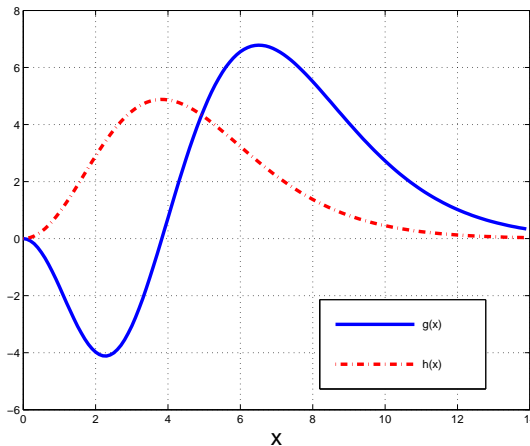


Fig. 1.4 The behaviour of $g(x)$ and $h(x)$ is illustrated.

where v_r is the peculiar velocity of the cluster and where $h(x) = x^4 e^x / (e^x - 1)^2$. In Fig. 1.4 the x -dependence of $g(x)$ and $h(x)$ is illustrated. Notice the $g(x)$ gives a fair approximation for the spectral distortion only if the temperature of the electrons is sufficiently small. In practice this happens for $T_e < 5$ KeV. When $T_e > 5$ keV the inclusion of relativistic corrections is mandatory. Such an inclusion will also correct the cross-over frequency since x_0 inherits relativistic corrections going as T_e/m_e .

1.6 Cosmological parameters

In recent years, thanks to combined observations of CMB anisotropies [35, 36], large scale structure [57, 58], supernovae of type Ia [59], big-bang nucleosynthesis [60], some kind of paradigm for the evolution of the late time (or even present) Universe emerged. It is normally called by practitioners Λ CDM model or even, sometimes, “concordance model”. The terminology of Λ CDM refers to the fact that, in this model, the dominant (present) component of the energy density of the Universe is given by a cosmological constant Λ and a fluid of cold dark matter particles. The cosmological constant (or more generally the dark energy) interacts only gravitationally with the other (known) particle species such as baryons, leptons, photons. In the present section we are going to anticipate a portion of the notions which will be discussed later in this book. The main purpose of this strategy is to give some empirical evidence of some of the assumptions (or even conjectures) that will be later on spelled out more clearly. In this perspective, for the moment, the Λ CDM model is simply the Standard Cosmological Model (which will be thoroughly introduced in chapter 2) completed by a (conventional) inflationary extension. By convention, here we mean a model where the only source of inhomogeneity is represented by scalar fluctuations of the geometry and vanishing contribution of the tensors.

According to this paradigm, our understanding of the Universe can be summarized in two sets of cosmological parameters: the first set of parameters refers to the homogeneous background, the second set of parameters to the inhomogeneities. So, on top of the indetermination on the (present) Hubble expansion rate, i.e. h_0 , there are various other parameters such as:

- the (present) dark energy density in critical units,^o i.e. $h_0^2 \Omega_{\Lambda 0}$;

^oInstead of giving the critical fraction of the total energy density alone, it is common practice to multiply this figure by h_0^2 so that the final number will be independent of h_0 .

- the (present) cold dark matter (CDM in what follows) energy density, i.e. $h_0^2\Omega_{c0}$;
- the (present) baryon energy density, i.e. $h_0^2\Omega_{b0}$;
- the (present) photon energy density (already introduced) $h_0^2\Omega_{\gamma 0}$;
- the (present) neutrino energy density, i.e. $h_0^2\Omega_{\nu 0}$;
- the optical depth at reionization (denoted by ϵ but commonly named τ which denotes instead, in the present book, the conformal time coordinate, see section 2);
- the spectral index of the primordial (adiabatic) mode for the scalar fluctuations n_s ;
- the amplitude of the curvature perturbations A_s ;
- the bias parameter (related to large scale structure).

To this more or less standard set of parameters one can also add other parameters reflecting a finer description of pre-decoupling physics:

- the neutrinos are, strictly speaking, massive and their masses can then constitute an additional set of parameters;
- the dark energy may not be exactly a cosmological constant and, therefore, the barotropic index of dark energy may be introduced as the ratio between the pressure of dark energy and its energy density (similar argument can entail also the introduction of the sound speed of dark energy);
- the spectral index may not be constant as a function of the wave-number and this consideration implies a further parameter;
- in the commonly considered inflationary scenarios there are not only scalar (adiabatic) modes but also tensor modes and this evidence suggests the addition of the relative amplitude and spectral index of tensor perturbations,^P i.e., respectively, r and n_T .

Different parameters can be introduced in order to account for even more daring departures from the standard cosmological lore. These parameters include

- the amplitude and spectral index of primordial non-adiabatic perturbations;
- the amplitude and spectral index of the correlation between adiabatic and non-adiabatic modes;

^PThese two quantities will be specifically defined and computed in the case of conventional inflationary models. The interested reader may already consult chapter 10 (see, in particular, Eqs. (10.82) and (10.84) and derivations therein).

- a primordial magnetic field which is fully inhomogeneous and characterized, again, by a given spectrum and an amplitude.

This list can be easily completed by other possible (and physically reasonable) parameters. We just want to remark that the non-adiabatic modes represent a whole set of physical parameters since, as it will be swiftly discussed, there are 4 non-adiabatic modes. Consequently, already a thorough parametrization of the non-adiabatic sector will entail, in its most general incarnation, 4 spectral indices, 4 spectral amplitudes and the mutual correlations of each non-adiabatic mode with the adiabatic one. Having said this, it is important to stress that this book will not deal with the problem of data analysis (or parameter extraction from the CMB data). The purpose of the present script will be to use CMB as a guiding theme for the formulation of a consistent cosmological framework which might be in sight but which is certainly not fully understood.

It is useful to collect here some remarks on the values of the cosmological parameters that have been determined by analyzing different sets of data. This discussion has been partially approached in this chapter when we discussed, very briefly, the historical development of CMB physics. Since the theme reported in the present section might be a bit too specific, it could be skipped in the first reading of this script.

The WMAP 3-year [39] data have been combined, so far, with various sets of data. These data sets include the 2dF Galaxy Redshift Survey [62], the combination of Boomerang and ACBAR data [63, 64], the combination of CBI and VSA data [65, 66]. Furthermore the WMAP 3-year data can be also combined with the Hubble Space Telescope Key Project (HSTKP) data [67] as well as with the Sloan Digital Sky Survey (SDSS) [68, 69] data. Finally, the WMAP 3-year data can be also usefully combined with the weak lensing data [70, 71] and with the observations of type Ia supernovae^q(SNIa).

Each of the data sets mentioned in the previous paragraph can be analyzed within different frameworks. The minimal Λ CDM model with no cut-off in the primordial spectrum of the adiabatic mode and with vanishing contribution of tensor modes is the simplest concordance framework.^r Diverse completions of this minimal model are possible: they include the addition of the tensor modes, a sharp cut-off in the spectrum and so on and so forth.

^qIn particular the data of the Supernova Legacy Survey (SNLS) [72] and the so-called Supernova “Gold Sample” (SNGS) [73, 74].

^rThe terminology used in the present section assumes the knowledge of the physics which is actually the main theme of the present book.

All these sets of data (combined with different theoretical models) lead necessarily to slightly different determinations of the relevant cosmological parameters. To have an idea of the range of variations of the parameters the following examples are useful:

- the WMAP 3-year data alone [39] (in a Λ CDM framework) seem to favour a slightly smaller value $h_0^2\Omega_{M0} = 0.127$;
- if the WMAP 3-year data are combined with the “gold” sample of SNIa [73] (see also [74]) the favoured value is $h_0^2\Omega_{M0}$ is of the order of 0.134; if the WMAP 3-year data are combined with *all* the data sets $h_0^2\Omega_{M0} = 0.1324$.
- similarly, if the WMAP data alone are considered, the preferred value of $h_0^2\Omega_{b0}$ is 0.02229 while this value decreases to 0.02186 if the WMAP data are combined with all the other data sets.

The aforementioned list of statements refers to the case of a pure Λ CDM model. If, for instance, tensors are included, then the WMAP 3-year data combined with CBI and VSA increase a bit the value of $h_0^2\Omega_{b0}$ which becomes, in this case closer to 0.023.

In what follows a list of values will be presented. In all these tables the slight differences in the various cosmological parameters will be self-evident. Consider, to begin with, the case of the standard Λ CDM model with no tensor. Let us see what this model gives if analyzed in the light of the WMAP data *alone*. The results are:

$$\begin{aligned}
 h_0 &= 0.732_{-0.032}^{+0.031}, & n_s &= 0.958 \pm 0.016, & A_s &= (23.5 \pm 1.3) \times 10^{-10}, \\
 h_0^2\Omega_{b0} &= 0.02229 \pm 0.00073, & h_0^2\Omega_{c0} &= 0.1054_{-0.0077}^{+0.0078}, \\
 \Omega_\Lambda &= 0.759 \pm 0.034, & h_0^2\Omega_{M0} &= 0.1277_{-0.0079}^{+0.0080}, \\
 \sigma_8 &= 0.761_{-0.048}^{+0.049}, & \tau &= 0.089 \pm 0.030.
 \end{aligned}
 \tag{1.40}$$

In Eq. (1.40) the parameters τ and σ_8 determine, respectively, the optical depth of reionization^s and the amplitude of matter fluctuations (determined within linear theory) on a scale of $8h_0^{-1}$ Mpc. The quantities related to the only fluctuations of the geometry (which are the scalars, in the minimal Λ CDM model) are n_s (the scalar spectral index) and A_s (the scalar amplitude). Both quantities must be defined at a given scale which is conventionally chosen to be $k_p = 0.002$ Mpc⁻¹ and is called, in the jargon, *pivot*

^sAt the level of notations we stress that, in the following part of the book, the letter τ will denote the conformal time coordinate. Here, however, we prefer to use the standard notations for the benefit of the reader.

wave-number or simply *pivot scale*. Different choices for the pivot scale can be adopted, especially when not only the adiabatic mode is present in the game but also non-adiabatic modes (see chapter 8).

Suppose now to combine the WMAP data with *all* the available data stemming, respectively, from other CMB experiments, from LSS observations, from supernovae and from lensing. The result, always in the framework of the Λ CDM model, will be

$$\begin{aligned} h_0 &= 0.704_{-0.016}^{+0.015}, & n_s &= 0.947 \pm 0.015, & A_s &= (23.5 \pm 1.3) \times 10^{-10}, \\ h_0^2 \Omega_{b0} &= 0.02186 \pm 0.00068, & h_0^2 \Omega_{c0} &= 0.1105_{-0.0038}^{+0.0039}, \\ \Omega_\Lambda &= 0.732 \pm 0.018, & h_0^2 \Omega_{M0} &= 0.1324_{-0.0041}^{+0.0042}, \\ \sigma_8 &= 0.776_{-0.032}^{+0.031}, & \tau &= 0.073_{-0.028}^{+0.027}. \end{aligned} \quad (1.41)$$

Clearly there are slight differences in the determinations of some relevant cosmological parameters. For instance, the indetermination in the Hubble parameter, i.e. h_0 decreases (from Eq. (1.40) to Eq. (1.41)) by almost 3%. Furthermore $h_0^2 \Omega_{M0}$ increases by 1%. The spectral index gets more red.^t

If the WMAP data are combined with the data stemming from type Ia supernovae (and, in particular, with the gold sample [73, 74]) the cosmological parameters are determined to be, always in the framework of a Λ CDM model:

$$\begin{aligned} h_0 &= 0.701 \pm 0.021, & n_s &= 0.946 \pm 0.016, & A_s &= (24.4_{-1.4}^{+1.3}) \times 10^{-10}, \\ h_0^2 \Omega_{b0} &= 0.02230_{-0.00072}^{+0.00069}, & h_0^2 \Omega_{M0} &= 0.1349_{-0.0060}^{+0.0061}, \\ \Omega_\Lambda &= 0.724 \pm 0.026, & \sigma_8 &= 0.784_{-0.041}^{+0.042}, & \tau &= 0.079_{-0.029}^{+0.030}, \end{aligned} \quad (1.42)$$

which means that the combination with the data of type Ia supernovae implies a smaller value for h_0 and a slightly higher value for the rescaled critical fraction of matter. This trend is confirmed, in a non-trivial fashion, by combining the WMAP data with the supernova data stemming from the Supernova Legacy Survey [72]. In this case the obtained cosmological parameters are

$$\begin{aligned} h_0 &= 0.724 \pm 0.023, & n_s &= 0.950_{-0.017}^{+0.016}, & A_s &= (23.8 \pm 1.3) \times 10^{-10}, \\ h_0^2 \Omega_{b0} &= 0.02234_{-0.00074}^{+0.00075}, & h_0^2 \Omega_{M0} &= 0.1293 \pm 0.0059, \\ \Omega_\Lambda &= 0.752_{-0.024}^{+0.025}, & \sigma_8 &= 0.758 \pm 0.041, & \tau &= 0.085 \pm 0.030. \end{aligned} \quad (1.43)$$

^tIn the jargon we talk about red spectra (if the spectral index is smaller than 1), blue spectra (if the spectral index is larger than 1) and white (or scale-invariant spectra) if $n_s = 1$.

Up to now the model used to compare the data with the observations has been the simplest Λ CDM model. However, there are various other possibilities. Take, for instance, the case where a non-vanishing tensor component is allowed. This quantity will be denoted by r (see, in particular, chapter 10 for a derivation). The quantity named r denotes the ratio between the tensor and the scalar power spectrum produced in the framework of the same cosmological model. If only the WMAP data are used for the determination of the cosmological parameters we will have

$$\begin{aligned} h_0 &= 0.787 \pm 0.052, & n_s &= 0.984^{+0.029}_{-0.028}, & A_s &= (21.0^{+2.2}_{-2.3}) \times 10^{-10}, \\ h_0^2 \Omega_{b0} &= 0.02233 \pm 0.0010, & h_0^2 \Omega_{M0} &= 0.1195^{0.0094}_{-0.0093}, \\ r &= 0.65, & \Omega_\Lambda &= 0.803 \pm 0.040, \\ \sigma_8 &= 0.702 \pm 0.062, & \tau &= 0.090 \pm 0.031. \end{aligned} \quad (1.44)$$

It is clear from the reported figures that, when we allow for a tensor component, the values of the rescaled critical fraction of matter decreases, the cosmological constant increases and the Hubble parameter increases sharply. Compare, indeed, Eqs. (1.40) and (1.44) which both refer to the WMAP data alone but analyzed in the light of the two mentioned models, namely the Λ CDM with no tensors and the Λ CDM with a tensor component parametrized in terms of the tensor to scalar ratio.^u

This trend also depends upon which data sets are combined. For instance, suppose now we take the Λ CDM model with tensors and analyze it in the light of the WMAP data combined with the data of the Sloan Digital Sky Survey [68, 69]. The result will be:

$$\begin{aligned} h_0 &= 0.716 \pm 0.026, & n_s &= 0.964^{+0.020}_{-0.021}, & A_s &= (23.0^{+1.6}_{-1.5}) \times 10^{-10}, \\ h_0^2 \Omega_{b0} &= 0.02282^{+0.00080}_{-0.00081}, & h_0^2 \Omega_{M0} &= 0.1339^{0.0052}_{-0.0053}, \\ r &= 0.30, & \Omega_\Lambda &= 0.803 \pm 0.040, \\ \sigma_8 &= 0.781 \pm 0.034, & \tau &= 0.077^{+0.029}_{-0.030}, \end{aligned} \quad (1.45)$$

showing values of h_0 and $h_0^2 \Omega_{M0}$ and r which are substantially smaller than those reported in Eq. (1.44).

This discussion could be extended for various pages and this might even stimulate the interest of some readers for the so-called parameter estimation strategies. This topic is beyond the scope of the present book. Furthermore, the opinion of the author is that at the present stage, it seems really difficult to decide which is the best and most predictive model just on the basis of

^uAs with the scalar spectral amplitude, the tensor to scalar ratio is also normally assigned at the pivot scale k_p .

parameter estimation strategies. Indeed, in the present discussion, just two benchmark models have been quoted but there could be many others. Here is an approximate list of possibilities:

- Λ CDM alone with no tensors;
- Λ CDM with tensors;
- Λ CDM with a cut-off in the primordial scalar spectrum;
- Λ CDM assuming a quadratic inflaton potential with minimal inflationary duration (i.e. 60 e-folds);
- open CDM model.
- w CDM (i.e. CDM plus dark energy parametrized by a constant barotropic index);
- w CDM without perturbations induced by the dark energy;
- w CDM with perturbations induced by dark energy.

Notice that, in the above list, further possibilities can be obtained by combining the different items of the list. For instance it is possible to consider the case where we have w CDM in an open Universe, and so on and so forth. Furthermore, the aforementioned list may become even longer: the choices reported here are by no means exhaustive or fully comprehensive. While we shall get back more precisely on the assumptions of the Λ CDM model, it should be stressed that the only purpose of this discussion is to emphasize that observations, especially in cosmology, are never independent of the underlying model. Therefore, in this context, there are two possible approaches. The first one is to focus on the *minimal* model. By *minimal model* we mean the model with the fewer number of parameters which is consistent with all the sets of data mentioned at the beginning of this section. There is, however, a second approach. Namely the one of selecting a pivot model which is not minimal but which is guided by physical considerations. These two approaches are complementary but none of them is decisive unless data of different quality (i.e. laboratory data) will soon enlighten the observational situation.